SIMULATION OF WAVE BEAM BARRIER COLLISIONS AND ORTHOGONAL TEST MODIFICATIONS

*Wang Junjie, Guo Chao, Li Shouxin, Yang Xuexin, Wang Yu*0009-0001-0995-2046*
Department of Automotive Engineering, Hebei Institute of Mechanical and Electrical Technology
Xingtai 054000, Hebei, China
Email: WANGYU@hbjd.edu.cn ; xtxiaolong@163.com

Abstract - Waveform beam guardrails are commonly used protective device in road traffic safety. In order to analyze the protective effect of the three-curved waveform beam guardrail under different collision angles and collision speeds, collision simulations were conducted at vehicle speeds of 30 km/h, 50 km/h and 70 km/h. In order to further improve the crashworthiness of the corrugated beam guardrail at 70Km/h, a four-factor three-level orthogonal test scheme was designed. The finite element analysis results show that the protective effect of the corrugated beam guardrail at a speed of 70km/h has decreased. After improvement, it was found that when the thickness of the guardrail beam is 4mm, the thickness of the energy-absorbing block is 4.5mm, the thickness of the post is 5mm and the post spacing is 2800mm, the maximum dynamic deformation of the guardrail is minimized, and good improvement effects can still be achieved for collisions at a speed of 70km/h, which further improved the anti-collision performance.

Keywords: W-beam Guardrails, Collision Simulation, Orthogonal Test, Finite Element Method, LS-DYNA

1. Introduction

W-beam guardrails are a commonly used type of safety barrier in traffic safety applications. Utilizing finite element analysis (FEA) for collision simulation to study the performance of W-beam guardrails offers advantages of low cost and high efficiency [1, 2]. Numerous studies have demonstrated a high degree of correlation between full-scale collision simulation results and experimental data, indicating that the application of LS-Dyna for simulating full-scale models possesses significant practical value [3]. Current systematic evaluation methods for vehicle collision protection effects assess deformation, vehicle acceleration, energy absorption capacity of the barriers, and dynamic vehicle responses [4, 5]. Investigating the collision protection capabilities of W-beam guardrails can enhance the passive safety performance of vehicles and drivers following a collision incident [6, 7]. Conventional research on collision safety indicates that W-beam guardrails perform well in low-speed scenarios. However, extensive studies reveal that as vehicle speed increases, the safety performance of W-beam guardrails declines sharply [8-10]. Therefore, there is a pressing need to enhance and improve the performance of W-beam guardrails. Given the numerous factors that affect their performance, it is essential to conduct collision simulations and orthogonal experimental design to better assess the collision safety of W-beam guardrails [11], aiming to achieve optimal design dimensions and configurations for these barriers.

2. Establishment of the Finite Element Model of the Guardrail

In 2017, China implemented a new corrugated beam guardrail structure [12, 13], as illustrated in Figure 1, with dimensions provided in Table 1. The material type of the corrugated beam guardrail is Q235.

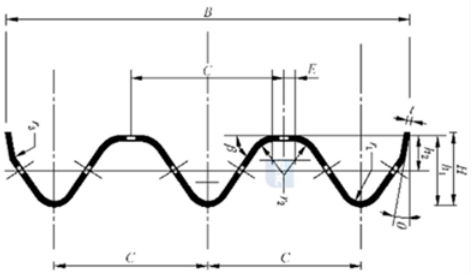

Figure 1: Dimensions of the three-bend waveform beam plate.

Table 1: Geometric dimensions of the waveform beam plate

Structural parameters	Value
B/mm	506
H/mm	85
t/mm	4
h1/mm	83
h2/mm	42
C/mm	194
E	14

r1	24
r2	24
r3	10
α	55
β	55
θ	10

In the simulation, the geometric model of the three-bend waveform beam plate is imported into LS-Pro for preprocessing. The model type is surface, so shell elements are used. With a section thickness set to 4.5 mm, material properties for Q235 steel, including elastic modulus, Poisson's ratio and density are defined in the software. A cell size of 30mm is set for meshing, resulting in a finite element mesh model with 23,206 elements and 24,168 nodes, as shown in Figure 2.

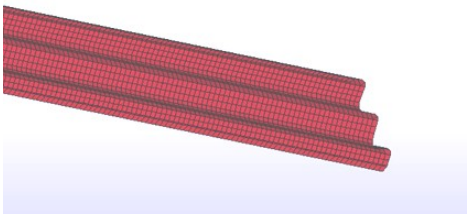

Figure 2: Finite element mesh model of the three-bend waveform beam plate

The complete structure of the guardrail consists of a three-bend waveform beam steel plate, hexagonal energy-absorbing blocks, and circular posts (as shown in Figure 3). Each component is connected by high-strength bolts. The energy-absorbing block is positioned between the waveform beam plate and the post, providing effective energy absorption. When a vehicle collides with the guardrail, the block experiences compressive forces, leading to deformation that effectively absorbs the impact energy. The energy-absorbing block has an overall shell structure with a hexagonal cross-section, a vertical height of 400 mm, and a wall thickness of 4.5 mm, as detailed in Figure 4.

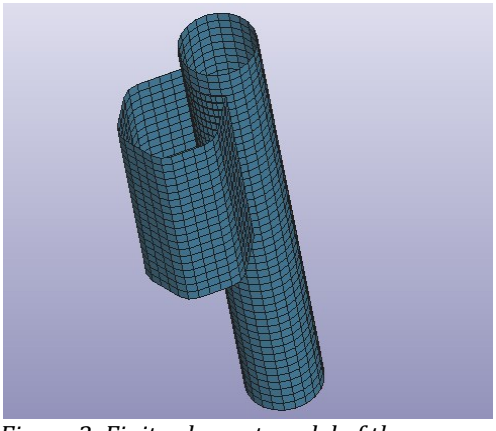

Figure 3: Finite element model of the energy-absorbing block and the post

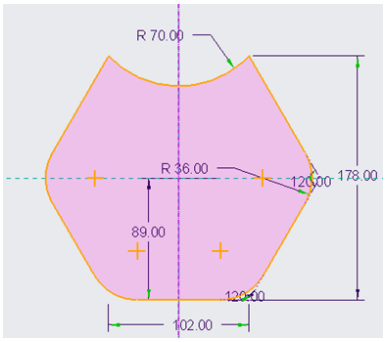

Figure 4: Dimensions of the energy-absorbing block

The post is connected to the ground and has a cir cular shell structure with a thickness of 4.5 mm and a diameter of 140 mm. The total height of the post is 2350 mm, with 1400 mm embedded in the ground. A fter assembling the energy-absorbing blocks with th e posts, the model is imported into LS-ProPost. A tot al of 5 waveform beam plates are set, resulting in 6 c ombinations of energy-absorbing blocks and posts. T he overall finite element model of the waveform guar drail is shown in Figure 5. Since the high-strength bo lts are ignored, automatic single surface contact (*CO NTACT_AUTOMATIC_SINGLE_SURFACE) is set to sim ulate the connection between the energy-absorbing blocks and the posts. After meshing, the energy-abso rbing blocks and posts have a total of 10,056 element s and 10,374 nodes.

Figure 5: Finite element model of the waveform guardrail

- ***Establishment of the Finite Element Model of the Vehicle***

When a small car collides with the guardrail, the primary contact surface is the exterior of the vehicle. Therefore, simplifying certain non-load-bearing components within the car does not affect the simulation results and can reduce computation time. In this study, a simplified meshing approach is applied to the selected small car finite element model. Given the complexity of the car model, with numerous parts making modelling challenging, a finite element model of a specific vehicle from a collision analysis platform is used. This model comprises 373 components, 271,147 elements, and 283,909 nodes, as shown in Figure 6.

Figure 6: Finite element model of the vehicle

The total weight of the vehicle is 1.32×10^3 kg, with a surface area of 5.3×10^7 mm^2. The vehicle's total length is 4350 mm and its width is 1398 mm. Detailed vehicle parameters are shown in Table 2.

Table 2: Vehicle parameters

Parameters	Value
Length × width × height /mm	4350×1698×1260
Volume/mm^3	2×10^9
Total mass /t	1.32
Surface area/mm^2	5.3×10^7
Material type	1*MAT ELASTIC 7*MAT BLATZKO RUBBER 20*MAT RIGD 24*MATPECEWISEINEAR PLASTICITY 26*MAT HONEYCOMB 63*MATCRUSHABLEFOAM
Cell type	*SECTION BEAM *SECTION SHELL *SECTION SOLID

- ***Establishment of the Coupled Finite Element Model of the Vehicle and Guardrail***

After completing the model processing for the waveform beam guardrail, the finite element model files (k files) of the guardrail and the vehicle are imported into LS-ProPost for coupling. For simplification in the calculations, the following assumptions are made:

For the three-bend waveform beam guardrail, the original bolt connections between the waveform beam plate and the energy-absorbing blocks, as well as between the blocks and the posts, are treated as welded connections for ease of computation. Thus, surface-to-surface welding contact (*TIED_SURFACE_TO_SURFACE) is applied between the waveform beam plate and the energy-absorbing blocks, as well as between the blocks and the posts.

For the contact between the vehicle and the guardrail, components like the vehicle's bumper and hood are created as a single PART, with automatic surface-to-surface contact (*AUTOMATIC_SURFACE_TO_SURFACE) established between this PART and the guardrail beam plate.

The static friction coefficient is set to 0.18, and the dynamic friction coefficient is set to 0.15. The coupled model of the vehicle and guardrail is shown in Figure 7.

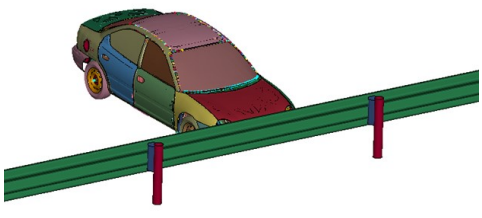

Figure 7: Coupled model of the vehicle and guardrail

3. Deformation Analysis of the Finite Element Simulation Results

- ***Collision condition at a speed of 30 km/h***

As shown in Figure 8, the displacement conditions of the guardrail under different collision angles with the vehicle at a speed of 30 km/h are illustrated.

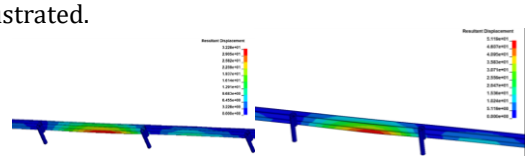

a) Collision angle of 5° b) Collision angle of 10°

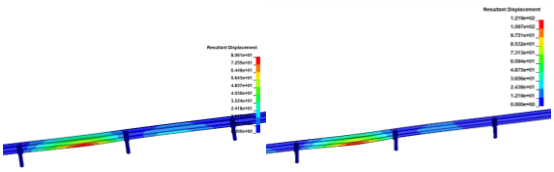

c) Collision angle of 15° d) Collision angle of 20°

Figure 8: Displacement Cloud Map of the Guardrail at a Collision Speed of 30 km/h

As shown in Figure 8a), when the collision angle is 5°, the maximum displacement of the guardrail is 32.28 mm, with a relatively small deformation. The maximum deformation occurs at the midpoint between the two block-outs, and the guardrail effectively performs its protective and guiding functions. In Figure 8b), at a collision angle of 10°, the maximum deformation of the guardrail reaches 51.19 mm, with minor deformation of the block-outs, while still fulfilling its protective and guiding roles. Figure 8c) illustrates that at a collision angle of 15°, the maximum deformation occurs at the center of the w-beam, reaching 80.61 mm, with slight deformation of the block-outs; the guardrail continues to provide protection and guidance. In Figure 8d), at a collision angle of 20°, the maximum deformation also occurs at the center of the w-beam, with a maximum displacement of 121.9 mm and minimal deformation of the block-outs, while the guardrail maintains its protective and guiding functions. At a collision speed of 30 km/h, the vehicle slows down and returns to its normal trajectory under the influence of the guardrail, demonstrating good protective effectiveness.

- ***Collision condition at a speed of 50 km/h***

The displacement conditions of the guardrail under different collision angles with the vehicle at a speed of 50 km/h are illustrated. In Figure 9a), with a collision angle of 5°, the maximum displacement of the guardrail is 35.11 mm, with relatively small deformation occurring at the midpoint between the two block-outs, effectively providing protection and guidance. Figure 9b) indicates that at a collision angle of 10°, the maximum deformation is 66.12 mm,

with minor deformation of the block-outs, maintaining protective and guiding functions. In Figure 9c), at a collision angle of 15°, the maximum deformation reaches 130 mm at the center of the w-beam, with slight deformation of the block-outs, while still achieving protection and guidance. Figure 9d) shows that at a collision angle of 20°, the maximum deformation is 232.8 mm at the center of the w-beam, with the block-outs deforming under impact, yet the guardrail continues to fulfill its protective and guiding roles. At a collision speed of 50 km/h, the guardrail exhibits smaller deformations at angles of 5°, 10°, and 15°, while a larger deformation occurs at 20°, yet the vehicle can still return to the normal road, demonstrating the guardrail's effective protective capability.

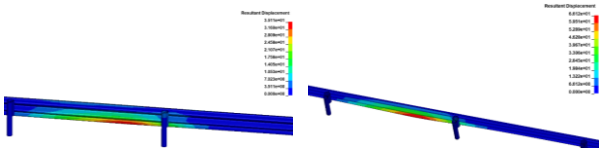

a) Collision angle of 5° b) Collision angle of 10°

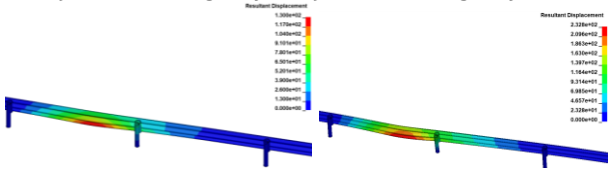

c) Collision angle of 15° d) Collision angle of 20°
Figure9: Displacement Cloud Map of the Guardrail at a Collision Speed of 50 km/h

- ***Collision condition at a speed of 70 km/h***

As shown in Figure 10, the displacement conditions of the guardrail under different collision angles with the vehicle at a speed of 70 km/h are illustrated.

When the collision angle is 5° (Figure 10a), the car collides with the post, resulting in a maximum deformation of 19.51 mm at the w-beam near the post, with relatively small deformation, allowing the guardrail to effectively provide protection and guidance. In Figure 10b), at a collision angle of 10°, the maximum deformation reaches 98.59 mm near the post, while the block-out shows minimal deformation, maintaining protective and guiding functions. Figure 10c) reveals that at a collision angle of 15°, the maximum deformation is 241.3 mm, with the block-out becoming flattened. In Figure 10d), at a collision angle of 20°, the maximum deformation reaches 384.1 mm near the post, where both the block-out and the post experience significant deformation. At a collision speed of 70 km/h, the guardrail shows small deformations at collision angles of 5° and 10°, while larger deformations occur at angles of 15° and 20°, with noticeable deformation of the block-outs and the post.

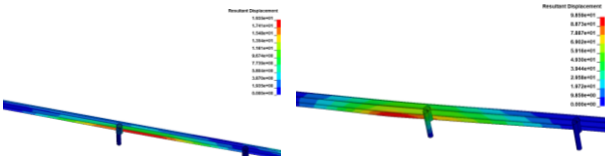

a) Collision angle of 5° b) Collision angle of 10°

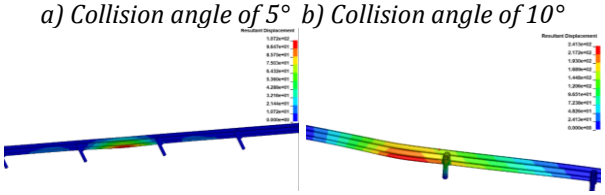

c) Collision angle of 15° d) Collision angle of 20°
Figure9: Displacement Cloud Map of the Guardrail at a Collision Speed of 70 km/h

Through the analysis, it is evident that at a vehicle speed of 70 km/h, the guardrail is prone to deformation. However, 70 km/h is a common driving condition, it is essential to optimize and improve this type of guardrail.

4. Orthogonal Experimental Design

By employing the orthogonal experimental method, comprehensive and efficient data can be obtained within a limited number of experiments [14]. The w-beam guardrail consists primarily of w-beams, posts, and energy-absorbing blocks, with variations in each component impacting the overall performance of the guardrail. During a vehicle collision with the guardrail, an increase in the thickness of the energy-absorbing block and posts initially results in a gradual increase in peak acceleration, followed by a rapid increase. This phenomenon occurs because increased thickness effectively enhances overall stiffness, leading to a rigidity-overload situation that diminishes energy absorption, causing acceleration to rise instead of decline. Consequently, in selecting the optimization scheme for the w-beam and energy-absorbing blocks, a thickness fluctuation of ±0.5 mm around 4 mm was chosen. The thickness of the posts was set above the standard to address snagging issues, as the primary cause of snagging during vehicle-guardrail interactions is lateral bending of the posts. To minimize lateral bending and reduce snagging, values within the range presented in Table 5-1 were selected. The spacing of the posts was based on the installation guidelines that recommend a distance of 2000 to 4000 mm, leading to the selection of three ranges from Table 5-1. The L9(3^4) orthogonal array was utilized for representation.

Based on the parameters of the A-class w-beam guardrail components, this study selected four factors: the thickness of the guardrail beam (A), the

thickness of the energy-absorbing block (B), the thickness of the post (C), and the post spacing (D). According to the structural parameters of the Q235 carbon steel guardrail, three levels were established for each factor. Table 3 presents the corresponding level values for each factor.

Table 3: Orthogonal Experiment Factors and Levels

Wave Beam Thickness A/mm	Energy-absorbing Block Thickness B/mm	Post Thickness C/mm	Post Spacing D/mm
3.5	3.5	5	2000
4	4	5.5	2800
4.5	4.5	6	3500

- ***Determine the optimal combination***

Table 4 presents a collision simulation of nine experimental schemes at a speed of 70 km/h and an angle of 15°. The analysis evaluates the safety performance of guardrails with different structural dimensions based on vehicle acceleration and the maximum dynamic response of the guardrails, with scheme 1 representing the parameters before optimization.

Table 4: Orthogonal Experimental Factor Level Combination Table

Test number	Combination levels	A	B	C	D
1	A1B1C1D1	1	1	1	1
2	A1B2C2D2	1	2	2	2
3	A1B3C3D3	1	3	3	3
4	A2B1C2D3	2	1	2	3
5	A2B2C3D1	2	2	3	1
6	A2B3C1D2	2	3	1	2
7	A3B1C3D2	3	1	3	2
8	A3B2C1D3	3	2	1	3
9	A3B3C2D1	3	3	2	1

Based on the level combinations shown in the table, a total of 9 experiments are required, with each vehicle model needing to collide with nine different types of barriers. Therefore, finite element simulation models will be established for each level to conduct collision simulation analysis for each type of barrier. Finite element models for nine different parameters of Q235 carbon steel barriers will be established according to Tables 3 and 4. The following images show the finite element collision models for barriers with distances of 3500mm, 2800mm, and 2000mm between the vehicle and the post.

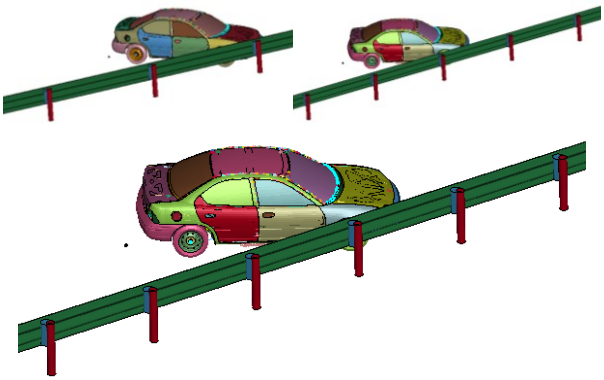

Figure 11 The barrier models with post distances of 3500mm, 2800mm and 2000mm

- ***Orthogonal Test Simulation Results***

To compare the protective performance of different specifications of barriers, the results of car collisions with nine different specifications need to be post-processed and organized, and curves depicting the maximum dynamic deformation of the barriers over time should be plotted. Below are the curves of the maximum dynamic deformation for Q235 carbon steel barriers during car collisions with varying specifications:

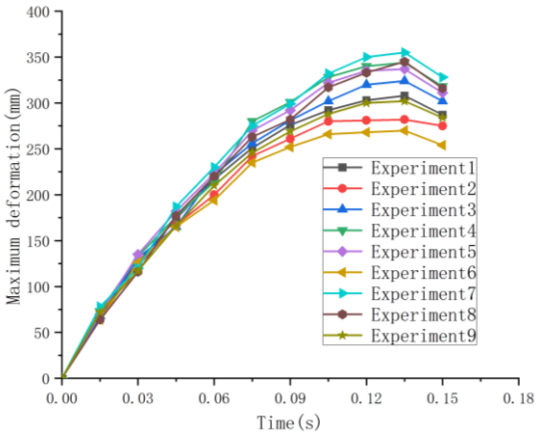

Figure 12: Time History Curve of Dynamic Deformation Amount

Before the collision time of 0.05 seconds, the deformation of the barriers before and after optimization is largely similar, with the wave beam primarily absorbing the impact from the vehicle at the start of the collision. By 0.13 seconds, the snagging process concludes, and the snagging phenomenon is not significant. The right front wheel of the vehicle exerts force on the side-bending post, causing the deformation to reach its maximum value. For the parameters of the barrier before optimization (Scheme 1), the maximum deformation is 308mm, while after optimization, it reduces to 270mm, representing a decrease of approximately 12.3%. From 0.13 to 0.15 seconds, adjacent posts

cause a rebound effect on the wave beam, resulting in a downward trend in the deformation curve.

In Figure 12, the maximum dynamic deformation values for all experimental schemes are below 400mm. Overall, the dynamic deformation of the barrier in experimental Scheme 6 is significantly reduced compared to the reference scheme. Specifically, Scheme 6 corresponds to the horizontal combination A2B3C1D2, with a wave beam thickness of 4mm, an obstacle block thickness of 4.5mm, a post thickness of 5mm, and a post spacing of 2800mm, resulting in the minimum maximum dynamic deformation.

Considering the stiffness of the barrier, the vehicle's composite acceleration, and the lateral deformation of the barrier, the optimal combination is ultimately determined to be A2B3C1D2: a wave beam thickness of 4mm, an obstacle block thickness of 4.5mm, a post thickness of 5mm, and a post spacing of 2800mm, which provides the best collision protection performance.

5. Conclusions

This paper employs finite element analysis to simulate the collision process of vehicles with wave beams. The effects of collision speed and angle on the barriers were studied, and the results indicate that:

（1）The three-bend wave beam demonstrates good elastic rebound characteristics under normal driving conditions at speeds ranging from 30 km/h to 70 km/h and collision angles of 5° to 20°. It effectively mitigates the impact force of the vehicle, preventing it from breaching the barrier or rolling over. However, at collision angles and speeds exceeding the set limits, the barrier may exhibit significant bending, fracturing, or even loss of protective capability.

（2）Under the conditions of speeds between 30 km/h and 70 km/h and angles of 5° to 20°, considering the stiffness of the barrier, the vehicle's composite acceleration, and the lateral deformation of the barrier, the optimal combination is ultimately determined to be A2B3C1D2. This configuration includes a wave beam thickness of 4mm, an obstacle block thickness of 4.5mm, a post thickness of 5mm, and a post spacing of 2800mm, resulting in the best collision protection performance.

References

[1] Ferdous, M. R., A. Abu-Odeh, R. P. Bligh, H. L. Jones, and N. M. Sheikh, 2011, Performance limit analysis for common roadside and median barriers using LS-DYNA: International Journal of Crashworthiness, v. 16, p. 691-706.

[2] Gutowski, M., E. Palta, and H. Fang, 2017, Crash analysis and evaluation of vehicular impacts on W-beam guardrails placed on sloped medians using finite element simulations: Advances in Engineering Software, p. S0965997817300182.

[3] Li, Z., H. Fang, J. Fatoki, M. Gutowski, and Q. Wang, 2021, A numerical study of strong-post double-faced W-beam and Thrie-beam guardrails under impacts of vehicles of multiple size classes: Accident Analysis & Prevention, v. 159, p. 106286.

[4] Matthew, Gutowski, Emre, Palta, Howie, and Fang, 2017, Crash analysis and evaluation of vehicular impacts on W-beam guardrails placed behind curbs using finite element simulations: Advances in Engineering Software.

[5] Yang, J., G. Xu, C. S. Cai, and A. Kareem, 2019, Crash Performance Evaluation of a New Movable Median Guardrail on Highways: Engineering Structures, v. 182, p. 459-472.

[6] HANG LIU, SHUAI GONG, SIYUAN LIU, et al. 2020, Research on the Modification of the Old W-beam Barrier on the Highway: Highway Engineering, ,45(6):173-180.

[7] RIHE Yao, HAIZHOU Xie, ZHENGJIE Wu, et al. 2024, Research on reconstruction and upgrading technology of corrugated beam guardrail: Highway, 69(06):263-266.

[8] WEN-BIN TANG, YONG-GANG TAI.2023, Influence of Thickness of Protective Layer on Performance of Class 4 W-beam Barrier under Narrow Shoulder Condition: Journal of Highway and Transportation Research and Development,,40(7):170-175.

[9] Wan Yanan. 2023, Research on Collision Modelling and Simulation Optimization of Wave Beam Barriers on High-Speed Highways: Northeast Forestry University, Transportation Engineering.

[10] DEWANG ZHAO, WANTING WANG, YUN XING, et al.2023, Research on the Crashworthiness and Lightweight of Highway Wave-beam Guardrail: Journal of Anhui University of Science and Technology(Natural Science),43(4):19-25.

[11] Li Tao, Xu Qingchao, Wang Guan.2022 Optimization of Deformation Control Indicators for Class SA Wave Beam Barriers in Central Medians : China Highway,(23): 96-101.

[12] People's Republic of China Industry Standard. 2017, Design Specifications for Highway Traffic Safety Facilities: Beijing: People's Communications Press.

[13] People's Republic of China Industry Standard. 2017, Design Guidelines for Highway Traffic Safety Facilities: Beijing: People's Communications Press.

[14] Shanghai People's Publishing House.1975 Orthogonal Experimental Design Method: Multi-Factor Experimental Method: Shanghai Science and Technology Exchange Station.